

Crystal Structure Analysis and Refinement using Integrated Intensities from Accurate Profile Fits*

G. Will

Mineralogical Institute, University Bonn,
5300 Bonn, West Germany.

Abstract

Careful experimental techniques, especially using synchrotron radiation facilities, give well resolved diffraction patterns. Remaining overlapping peaks can be separated by profile fitting and profile analysis. The derived parameters are: peak position for lattice constants, integrated intensities for crystal structure work and halfwidth for line broadening analysis. Crystal structure refinements with the powder least squares program POWLS yield R factors routinely around $R = 1.5\%$ and as low as $R = 0.6\%$. For actual structure analysis Fourier maps have been calculated in the case of the orthorhombic olivine analogue Mg_2GeO_4 . Another non-trivial example concerns CeO_2 , where chemical bonding features are derived. From an analysis of anomalous dispersion in Yb_2O_3 the correction terms f' have been derived as a function of energy for four wavelengths measured close to the L-absorption edge of Yb.

1. Introduction

A powder diffraction diagram contains full and complete information of the crystals under study. This statement holds equally well for X-ray diffraction, neutrons or synchrotron radiation. Also, from a general and theoretical point of view, there is in principle no difference between single-crystal data and powder diffraction data. The difficulties come about because in any powder diffraction diagram the Fourier transform of the crystals are superimposed in random orientations in reciprocal space and averaged for equal D^* values. This naturally is a serious handicap in the data analysis and it naturally imposes constraints and limitations which cannot be overcome by mathematical procedures. For example, the effects of anomalous dispersion lead to a violation of Friedel's law, which is lost however in powder diffraction diagrams. Also in cubic systems, as another example, we have intrinsic overlaps of equal $h^2 + k^2 + l^2$, such as 511 and 333.

The refinement of crystal structures from powder diffraction data has attracted much interest during the last decade and it has today reached a state where in many cases it has become routine, especially if the structures are simple and straightforward and if the full pattern refinement method, as first proposed by Rietveld (1967, 1969), can be applied. In recent years much additional effort has been spent in making a more careful analysis of powder diffraction data and in extracting more information,

* Paper presented at the International Symposium on X-ray Powder Diffractometry, held at Fremantle, Australia, 20-23 August 1987.

especially information on more difficult problems and the analysis of low symmetry diffraction patterns.

This report is concerned with a procedure for analysing powder diffraction data in two consecutive and completely independent steps. It starts with a peak shape analysis followed by a profile analysis of the diffraction diagram, both of which do not require either knowledge or information on the material under study. In a superficial way this may be considered a 'black box' as far as the crystal structure is concerned. With this information at hand any further calculation and analysis of crystal properties can be done. These are mostly crystal structure refinements or determinations of lattice constants, but also careful and sophisticated line broadening analysis for particle size or strain/stress analysis can be done quite easily. The most important point, however, is the complete separation of peaks even if they strongly overlap. This means we are approaching single crystal equivalent data, which we can use for Patterson mapping, for Fourier calculations and also for chemical bonding analysis in the nomenclature of high order/low order analysis.

2. Peak Shape Analysis

Any measured diffraction pattern originates from the true diffraction effects of the specimen, which may be idealised by a delta-function convoluted with a function describing possible line broadening. Both effects are superimposed on the geometrical and instrumental aberrations including the intensity distribution of the radiation source. The observed experimental diffraction spectrum is therefore the convolution of the instrumental contributions (G for geometrical) and the Bragg scattering from the specimen (S). This is superimposed, i.e. added to the background scattering (BG):

$$Y(2\theta) = G*S + BG. \quad (1)$$

In order to perform a profile analysis, the shape of a single well-behaved diffraction peak, e.g. the angular distribution of the data points Y_i around the centre line at $2\theta_p$, has to be known. Especially when sealed X-ray tubes are used, this shape function is complicated and cannot be determined and analysed in a straightforward way. A number of functions have been proposed and are presently used in Rietveld programs (Young and Wiles 1982), but none however is suited to describe the pattern properly. A different approach has been put forward by Huang and Parrish (1975) by describing the α_1, α_2 doublet by seven Lorentzian (L) functions (3L for α_1 , 3L for α_2 and the seventh for α_3). The angular dependence of the peak shape in this setup varies strongly with 2θ and has to be determined at the beginning of an experimental adjustment by using standard materials, such as silicon etc. Details have been given by Will *et al.* (1983 *b*).

In neutron diffraction and also energy dispersive synchrotron experiments the line shape is Gaussian and therefore simple. Complications were encountered when we began using synchrotron radiation in an angular-dispersive mode of the conventional powder diffraction, e.g. when we worked with monochromatised synchrotron radiation. Over three runs in 1985 (Will *et al.* 1987 *a*), in 1986 (Will *et al.* 1988), and again in 1987 at the Stanford Synchrotron Radiation Laboratory (SSRL) we experienced each time quite different profile shapes; for example, a double Gaussian function, a pseudo-Voigt function and, last but not least, a Lorentzian contribution shifted by

about 0.05° from the main Gaussian peak. This definitely makes profile analysis a serious and important matter for further success.

Let us now assume that we have derived (by trial and error) the correct profile function. Then we can proceed with the actual profile analysis of the diffraction diagram.

3. Profile Fitting Procedure—Profile Analysis of the Diffraction Pattern

In order to make the profile fitting procedure attractive to the average user and easy for the expert, it has to be automated as much as possible, but still leaving sufficient freedom to interact with the analysis. This can be done, certainly in principle, with modern computers and it should be done interactively. We have worked in this direction and written a package with several programs and choices.

As a first step the background has to be determined and subtracted. Since the principal sources of background—insufficient shielding, electronic noise and other physical effects—cannot be calculated in a general way, it must be determined by analytical procedures. Our program allows us to choose from two possibilities. We can lay a polygon fit either through manually selected footing marks in the powder pattern or we can call for a fully automatic procedure, which places a background line in the diagram. This method is based on an algorithm by Steenstrup (1981). Thereby, we fit a polynomial of degree $n < 15$ through the total assemblage of the data points in the diagram and gradually arrive in an iterative mode at the true background (for details see Jansen *et al.* 1988).

There is a choice in our program system of subtracting the background from the diffraction pattern leaving a diagram without background for further analysis. This is sometimes helpful, especially if the background is high. Further, we can smooth the data by a spline function (Savitzky and Golay 1964).

For the actual profile analysis we have three choices of fitting, which are handled by the programs PROFAN, PROFIL and FULFIT.

PROFAN is an interactive program which is designed for on-line operation (in the IBM VMS version) using a graphic display. By moving the cursor the diagram can be segmented into smaller sections, which are then separately analysed one after another. Within one segment the starting values are again selected by moving the cursor to a peak position (or a shoulder of a suspected peak). By pressing ENTER the peak position, the peak height and the profile shape function (taken from a library) are entered into the computer for each peak wanted. The FWHM data are taken from the library, where also various profile shape functions are stored. Other functions can be easily implemented. The quality of the fitting (which is done within seconds) and the profile R factors reveal whether all peaks are accounted for or not. This program is especially useful if multiphase data have to be analysed, or if there are impurities in the diagram. It is of specific importance in neutron diffraction if incommensurate magnetic structures with weak satellites have to be analysed (see Fig. 1).

PROFIL is a fully automatic peak finding and profile refining program. Peak search is here performed by calculating higher order derivatives of the experimental profiles, based on a deconvolution algorithm according to Steinier *et al.* (1972). Minima in the second derivative and maxima in the fourth derivative curve indicate starting positions $2\theta_p$ for the final profile refinement.

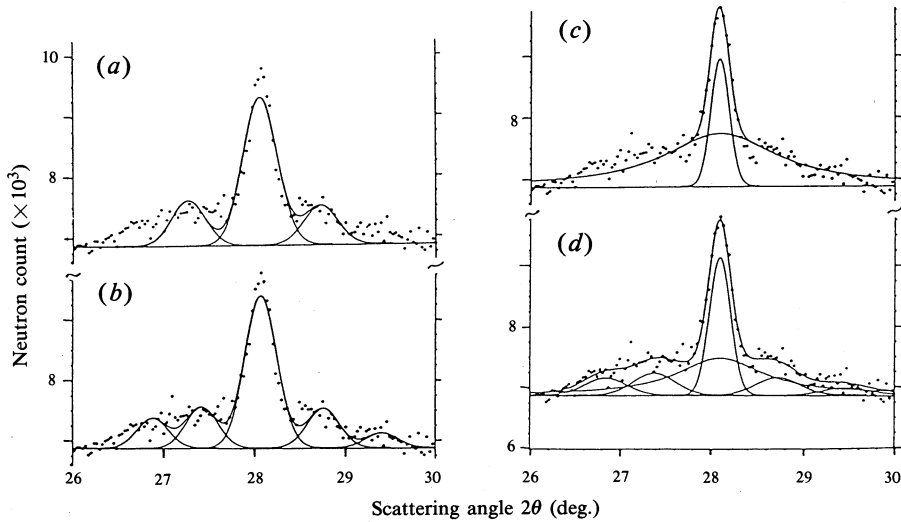


Fig. 1. Example of profile analysis from a neutron diffraction diagram of $\text{Tb}_{0.33}\text{Y}_{0.67}\text{Ag}$ (taken at 16 K) for the 111 reflection. The following profile models were used:

(a) Central peak with one satellite on each side. Gaussian profiles, with satellite halfwidths constrained; $R_{\text{pf}} = 3.3\%$.

(b) Central peak with two satellites. Gaussian profiles, with satellite halfwidths constrained; $R_{\text{pf}} = 2.2\%$.

(c) Central Gaussian peak sitting on a Lorentzian shaped diffuse background; $R_{\text{pf}} = 2.0\%$.

(d) Central peak with two satellites of Gaussian profile, with satellite halfwidths constrained. This quintet is now sitting on a Lorentzian shaped background; $R_{\text{pf}} = 1.6\%$. Part (d) is basically (b) + (c), and is the final model.

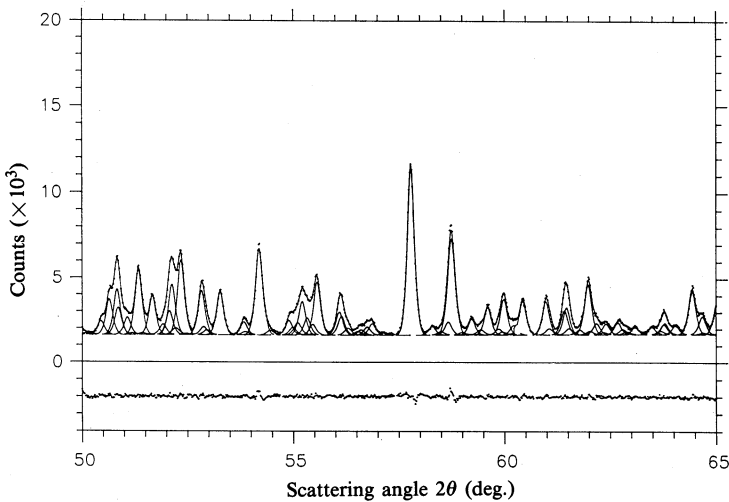


Fig. 2. Example of a FULFIT diagram from olivine with synchrotron radiation, showing the section $2\theta = 50^\circ\text{--}65^\circ$. The R profile is 1.5%.

The most advanced program system is FULFIT, which comes very close to the total pattern refinement procedure by Rietveld (1967, 1969), being short only of the crystal structure refinement. It needs as starting values only the instrumental parameters for the halfwidth, and starting values for the lattice parameters (including crystal system and Laue group). The program generates a list of hkl values and d spacings, with the extinctions given by the Laue group as input data, then calculates and refines the peak positions and peak heights for each reflection. The lattice parameters are calculated and refined in an iterative way from the peak positions. The final output is integrated intensities of the individual hkl , their standard deviations and correlations, refined values for the lattice parameters and, if required, in the last cycle refined values for R , S and T , the constants in the Cagliotti description (Cagliotti *et al.* 1958) of the FWHM. Further, the zero angle value $2\theta_0$ and, if desired, a value for λ are determined. Of specific importance are the standard deviations and the correlations, which are needed for further crystal structure refinement in POWLS. Fig. 2 gives an example.

In all three programs we minimise the equation

$$M = \sum_i w_i (Y_i^{\text{calc}} - Y_i^{\text{obs}})^2, \quad (2)$$

where w_i are the weights given to each observation Y_i . A linearisation is reached by a Taylor series expansion (for further details we refer to Jansen *et al.* 1988).

4. Structure Refinement with POWLS

The integrated intensities from the foregoing profile refinements are used as input values for crystal structure refinement in the second stage. We use here a sophisticated and especially well-developed program POWLS, developed originally by Will (1979) and in the meantime repeatedly enhanced and improved (Will *et al.* 1983*a*). This has been described in several papers, with many examples published, and here we will not go into further details. Values for R factors (R -Bragg) around 1% or lower can be obtained. The function to be minimised in POWLS is given by the following equation, similar to (2):

$$M = \sum_i w_i \{ I_i^{\text{obs}}(hkl) - (1/K) I_i^{\text{calc}}(hkl) \}^2. \quad (3a)$$

Now, however, the matrix of the residuals is defined by the linearised differences between observed and calculated integrated intensities (Jansen *et al.* 1988). The linearisation of the residuals is done again by a Taylor series expansion. Here K is the scale factor and w_i are the appropriate weights based on the estimated standard deviations of the integrated intensities, where $w = 1/\sigma^2$ and

$$\sigma = 0.5(I^{\text{obs}})^{\frac{1}{2}} + \text{const.} \quad (3b)$$

The constant is adjusted to the observed data.

One further correction deserves attention, namely preferred orientation. This is one of the three main errors in a structure refinement not concerned with the structure itself (the other two are the peak shape function and the proper background correction). Even a very experienced scientist will not succeed in preparing a sample which has a complete random distribution of particles. This effect of non-randomness

is corrected in POWLS in the course of the crystal structure refinement by using the term GP in calculating the intensity of the model structure:

$$I^{\text{calc}}(\text{corr}) = I^{\text{calc}} \exp(-GP\phi^2), \quad (4)$$

where ϕ is an acute angle between the diffraction plane and the selected preferred orientation plane (Will *et al.* 1987*a*). In all cases the quality of the refinement is defined by R values and by goodness of fit figures, as is common practice.

5. Crystal Structure Analysis from Profile Fitted Data

The rapid advancement of synchrotron radiation facilities has made experiments more feasible, and powder diffraction diagrams have improved in appearance. For example, the FWHM was $0.17^\circ 2\theta$ in 1985 (Will *et al.* 1987*b*) at Stanford. With the use of a 365 mm long collimator we could increase the resolution of the powder diffraction diagrams and reach a FWHM of 0.07° in 1986 (Will *et al.* 1988). In a different technique with a Ge monochromator behind the sample in the diffracted beam, Hastings *et al.* (1984) could even get a FWHM of 0.01° , however, at the expense of intensity or time. Such diagrams exhibit well-resolved peaks and are well suited for further analysis. Some remaining overlapping peaks can be separated by the foregoing profile analysis methods without difficulty. Therefore, we are now in a position to do calculations similar to single crystal data. This of course requires that there is no intrinsic overlapping of reflections, as we experience for example in cubic systems, or in quartz. With low or lower symmetry diffraction patterns, such as orthorhombic systems, we can easily separate all peaks and then start calculating Patterson or Fourier diagrams.

(a) Electron Density Distribution in Mg_2GeO_4

We have examined Mg_2GeO_4 , an olivine analogue (Will and Lauterjung 1987). For this compound, single crystals are not available and therefore the analysis has to be done with powder methods. The diffraction data were collected at the Stanford facility. The experimental conditions were $\lambda = 1.74 \text{ \AA}$, a 2θ range of 18° – 85° , $\Delta(2\theta) = 0.01^\circ$, $t = 2 \text{ s}$, and total run time of about 4 hours.

Mg_2GeO_4 crystallises in the space group $Pbnm-D_{2h}^{16}$. The lattice parameters are $a = 4.9106(3)$, $b = 10.3214(6)$ and $c = 6.0365(3) \text{ \AA}$. With the greatly increased resolution and longer wavelength most of the peaks were well resolved and the others could be easily separated with profile fitting. In all 81 reflections were obtained; typical sections are shown in Fig. 3.

With this investigation we were able to go beyond solely structure refinement to actual structure analysis. We were able to calculate Fourier maps (electron density distributions) directly from the observed powder data. This could be done because the structure type was known, so we could immediately determine the phases for Fourier calculations. The calculation of Patterson maps would not have posed any difficulties but they were not needed. It should be noted that the Fourier coefficients were taken directly from the first stage of the analysis, i.e. after the profile refinement stage. Such a Fourier section is shown in Fig. 4*a* with a plane containing 01–Ge–02 of the GeO_4 tetrahedron. The Mg atoms are above the plane.

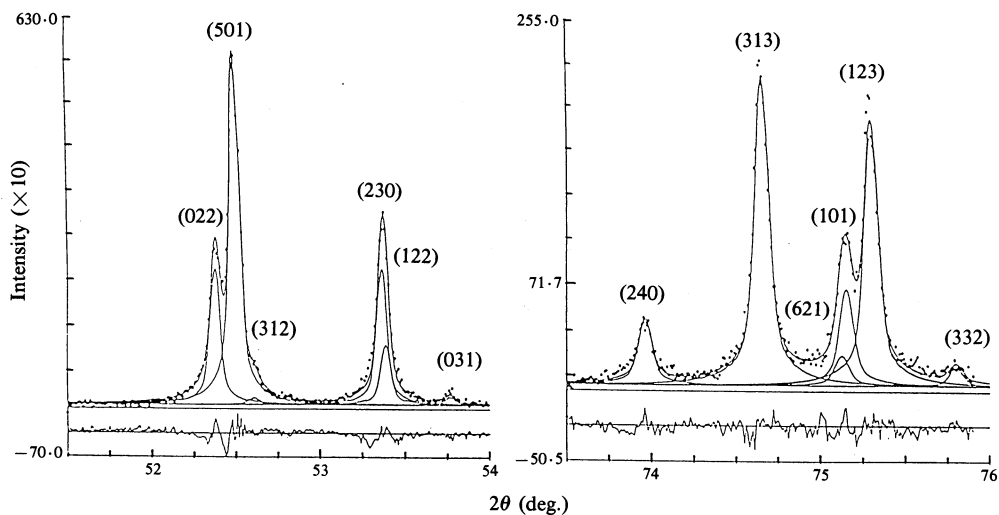


Fig. 3. Two profile fitted sections of Mg_2GeO_4 . Differences between experimental and calculated points are shown below each section. The resolution is 0.05° .

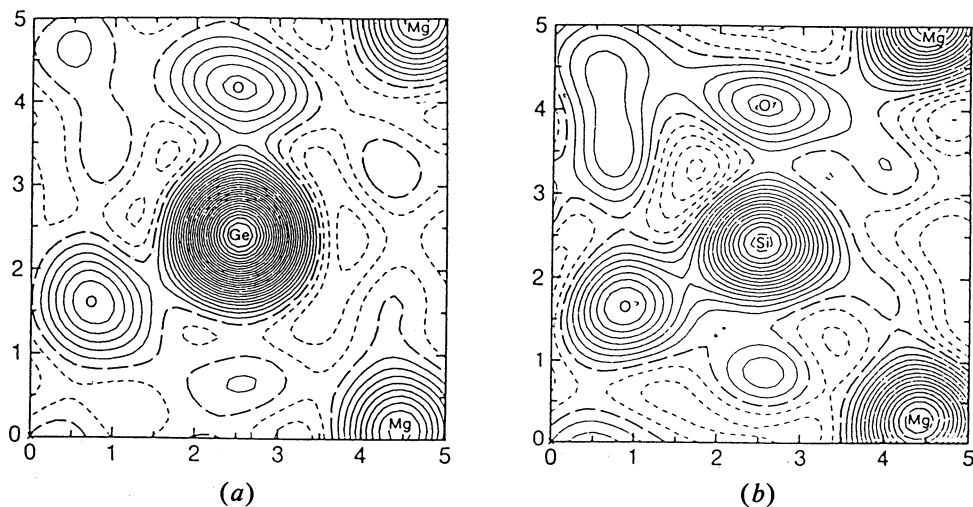


Fig. 4. Fourier map of (a) a section of Mg_2GeO_4 calculated from profile-fitted powder diffraction data and (b) $(\text{Mg}, \text{Fe})_2\text{SiO}_4$ a natural olivine calculated from single-crystal data.

It is now possible to compare results from powder diffraction directly with the isostructural silicate from a single crystal study. A detailed single crystal study was done on a natural olivine crystal $(\text{Mg}, \text{Fe})_2\text{SiO}_4$ with 10% Fe from San Carlos, Arizona. To obtain a direct comparison with the Mg_2GeO_4 powder data the single-crystal dataset containing 1349 reflections was reduced to the same reflections used in Fig. 4a, and is shown in Fig. 4b. The excellent agreement between the two maps is convincing demonstration of the power of the advanced methods of powder diffraction. The differences arise from the different scattering powers of Ge and Si.

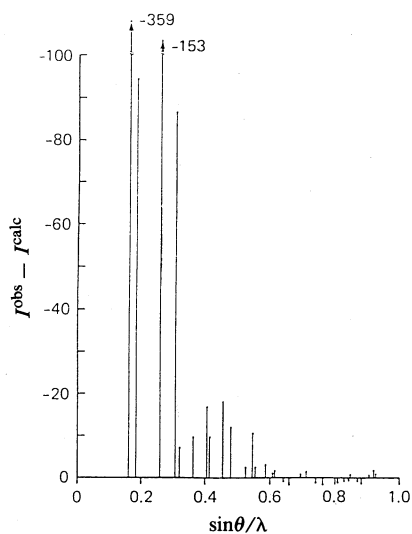


Fig. 5. Differences between observed and calculated intensities of CeO_2 determined from POWLS refinement.

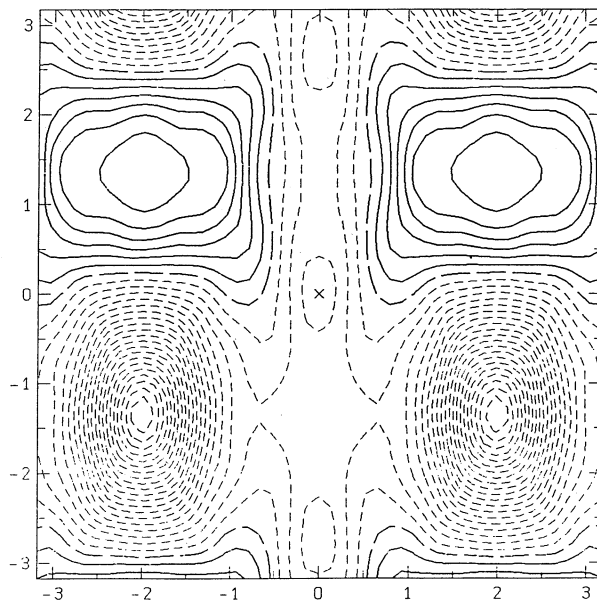


Fig. 6. Difference Fourier map of CeO_2 , calculated with the structure factor differences $F^{\text{obs}} - F^{\text{calc}}$, calculated from the intensities determined by POWLS. Fig. 6 is calculated from the intensity differences shown in Fig. 5.

(b) CeO₂

In cerium oxide we could analyse features of chemical bonding by separating the high angle data, sensitive only to the common crystal structure (atomic positions, temperature factors and scale factor), from the low angle data, which contain in

addition to the crystal structure also the deformation of the outer electrons due to chemical bonding. CeO_2 , a simple compound, crystallises in the CaF_2 -type structure with no positional parameters. A least squares refinement with all reflections, 32 peaks, some intrinsically overlapped from 52 hkl values, did, surprisingly for us, not go below $R = 2.64\%$. Inspection of the intensity differences $I^{\text{obs}} - I^{\text{calc}}$ revealed large deviations at small diffraction angles, e.g. in the low order (LO) region. The conclusion is that the compound is not a simple ionic crystal but has an appreciable covalent contribution. Based on our previous experience in the investigation of chemical bonding by high order (HO)/low order (LO) analysis (see e.g. Coppens 1977; Kirfel and Will 1980) we found very good agreement of the HO data with an R factor as low as 0.6% for the last 17 reflections with indices beyond $s = \sin \theta/\lambda = 0.6 \text{ \AA}^{-1}$. In the LO region, i.e. reflections before this limit, there was severe disagreement, as shown in Fig. 5. It is well known from single-crystal analysis that a refinement of the full dataset will absorb wrong chemical bonding features by wrong scale factors and wrong temperature factors. These parameters have to be assessed very accurately from the HO data alone. They can then be used to model the experimental LO (low angle) data. These data have to be known very accurately. It is the advantage of independent profile analysis that we could use the intensities in the

Table 1. Refined structure data for Yb_2O_3

Dataset	Wavelength (\AA)			
	1.3875	1.3895	1.3956	1.4150
f' (exp.)	-21.2(2)	-19.5(2)	-15.5(2)	-13.7(2)
f' (theor.)	-16.41	-14.42	-12.19	-9.86
Difference	4.8	5.1	3.3	3.8
a_0		10.436(1) ^A 10.4322(5) ^B		
$x(\text{Yb})$	-0.0322(1)	-0.0322(1) -0.03253(4)	-0.0321(1)	-0.0322(1)
$x(\text{O})$	0.3905(11)	0.3918(9) 0.3910(6)	0.3909(12)	0.3912(11)
$y(\text{O})$	0.1551(9)	0.1545(8) 0.1523(6)	0.1556(10)	0.1545(9)
$z(\text{O})$	0.3798(12)	0.3805(9) 0.3807(6)	0.3796(13)	0.3802(11)
$B(\text{Yb1})$	0.20(9)	0.12(6) 0.25	0.24(8)	0.15(6)
$B(\text{Yb2})$	0.06(5)	-0.03(3) 0.21	0.11(4)	0.08(3)
$B(\text{O})$	0.30(17)	0.48(18) 0.49	0.28(18)	0.24(17)
GPC ^C	0.061(10)	0.058(8)	0.067(10)	0.058(8)
$R(\text{Bragg})^{\text{D}}$ (%)	1.75	1.26	1.65	1.42
$wR(\text{Bragg})^{\text{E}}$ (%)	2.30	1.64 3.52 ^B	2.20	1.81

^A Average of four wavelengths.

^B Values in second line are from single-crystal data (Saiki *et al.* 1985).

^C Preferred orientation plane (111), see equation (4).

^D Using unit weights.

^E Using weighting scheme, see equation (3).

LO region to extract $|F|$ values and use them for $F^{\text{obs}} - F^{\text{calc}}$ synthesis. Fig. 6 shows an example. There is obviously a charge accumulation in the regions between the cesium ions. Placing point charges on these sites did improve the overall agreement appreciably from $R = 2.6\%$ to 1.7% , but nevertheless it does not yet fully describe the bonding features in the crystal. The analysis is not complete and we are now doing multipole refinement in order to fully describe the bonding behaviour.

(c) *Anomalous Dispersion in Yb_2O_3*

Anomalous X-ray scattering is well known as a powerful tool for estimating the phases in crystal structure analysis (Ramaseshan and Abrahams 1975). This method is used today mainly in macromolecular and protein structure determinations, where rare earth atoms show large anomalous scattering effects at their L edges. The use of the method for phase determination requires selecting a wavelength close to an absorption edge, with possibly several wavelengths to be used. Relativistic calculations of the anomalous scattering contributions f' and f'' cannot be done reliably at present, and therefore a direct experimental determination is required. This can best be done by single-crystal measurements which, however, require long

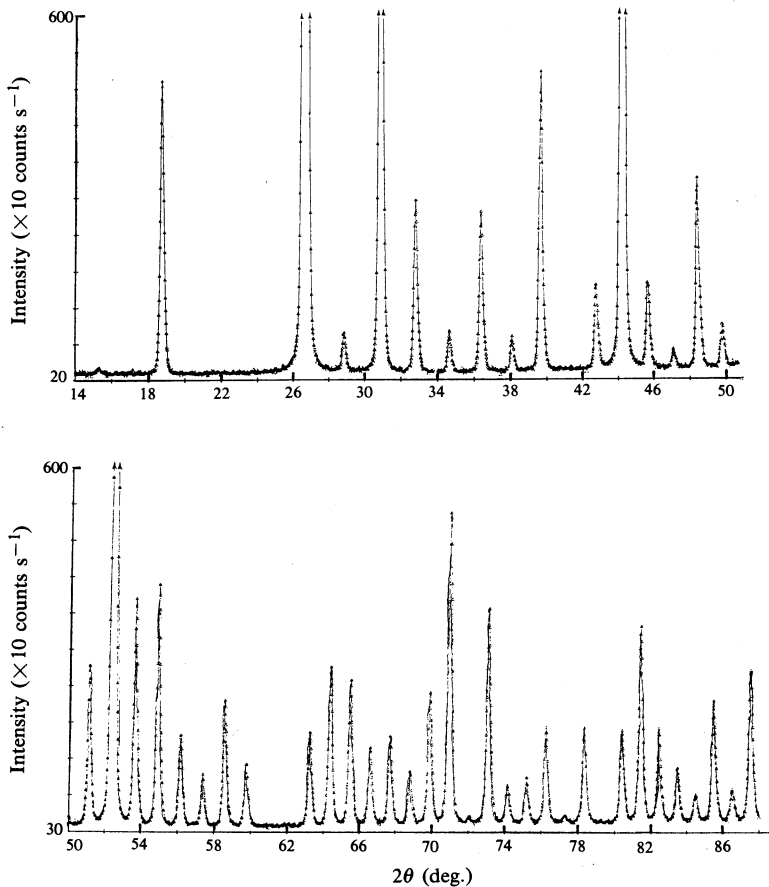


Fig. 7. Powder diffraction pattern of Yb_2O_3 , with synchrotron radiation, $\lambda = 1.3895 \text{ \AA}$, and resolution 0.17° . The highest peak intensity was 56600 counts per second for (222) at 26.7° .

measuring times. Therefore, powder methods would be most suitable. Synchrotron radiation is needed in either case. We have tested this possibility and measured Yb_2O_3 at four wavelengths (see Table 1) close to the L-adsorption edge of ytterbium in order to determine the values of f' .

Due to the intrinsic overlap of the Friedel pairs (hkl) and $(-h, -k, -l)$ in powder diagrams, it is not possible to determine the imaginary terms f'' . However, f'' can be calculated from f' by applying the Kramer–Kronig dispersion relation, and therefore even with this limitation the technique of powder diffraction and profile analysis is still very useful and powerful.

Yb_2O_3 crystallises in the space group $Ia\bar{3}-T_h^7$, and the structure type is $\alpha\text{-Mn}_2\text{O}_3$. The data analysis was done by POWLS least squares calculations. The diagrams were taken in the range $2\theta = 14^\circ\text{--}88^\circ$, and this yielded 44 to 48 well-resolved peaks (see Fig. 7), coming from 100 often intrinsically overlapping hkl planes. In the final runs R factors around 1.5% were obtained. The crystal structure values derived from the four datasets are consistent and well within the error limits, and they agree very well with a recent single-crystal study (Saiki *et al.* 1985).

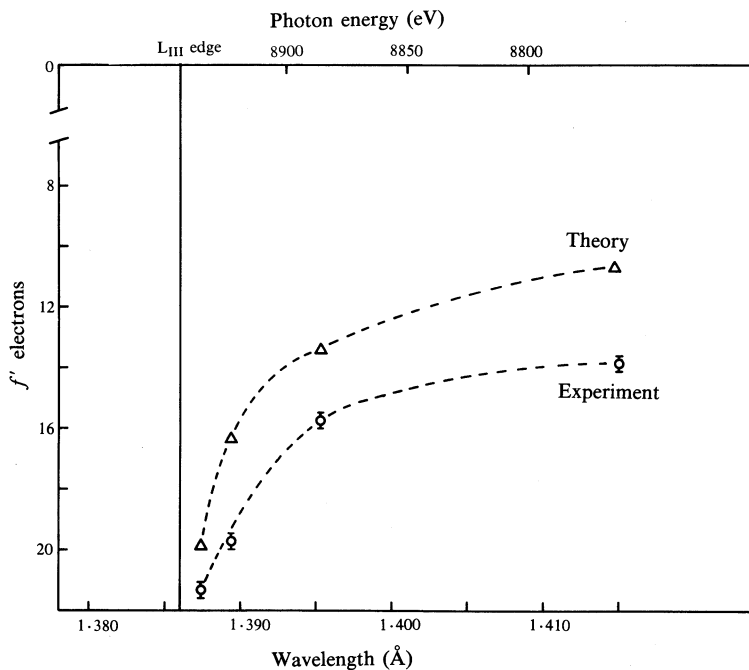


Fig. 8. Experimental and theoretical values of f' near the Yb L_{III} absorption edge.

The final results are shown in Table 1 and Fig. 8 (Will *et al.* 1987*a*). Included in Table 1 are the theoretical values for f' provided by D. Libermann (personal communication, 1986) using a modified and extended version of his earlier program (Cromer and Liberman 1970, 1981). The theoretical values are (in absolute terms) systematically smaller than the experimental ones. This is also the case for Sm and Gd measured by Templeton *et al.* (1980, 1982) from single-crystal data and it demonstrates the importance of deriving the f' values experimentally.

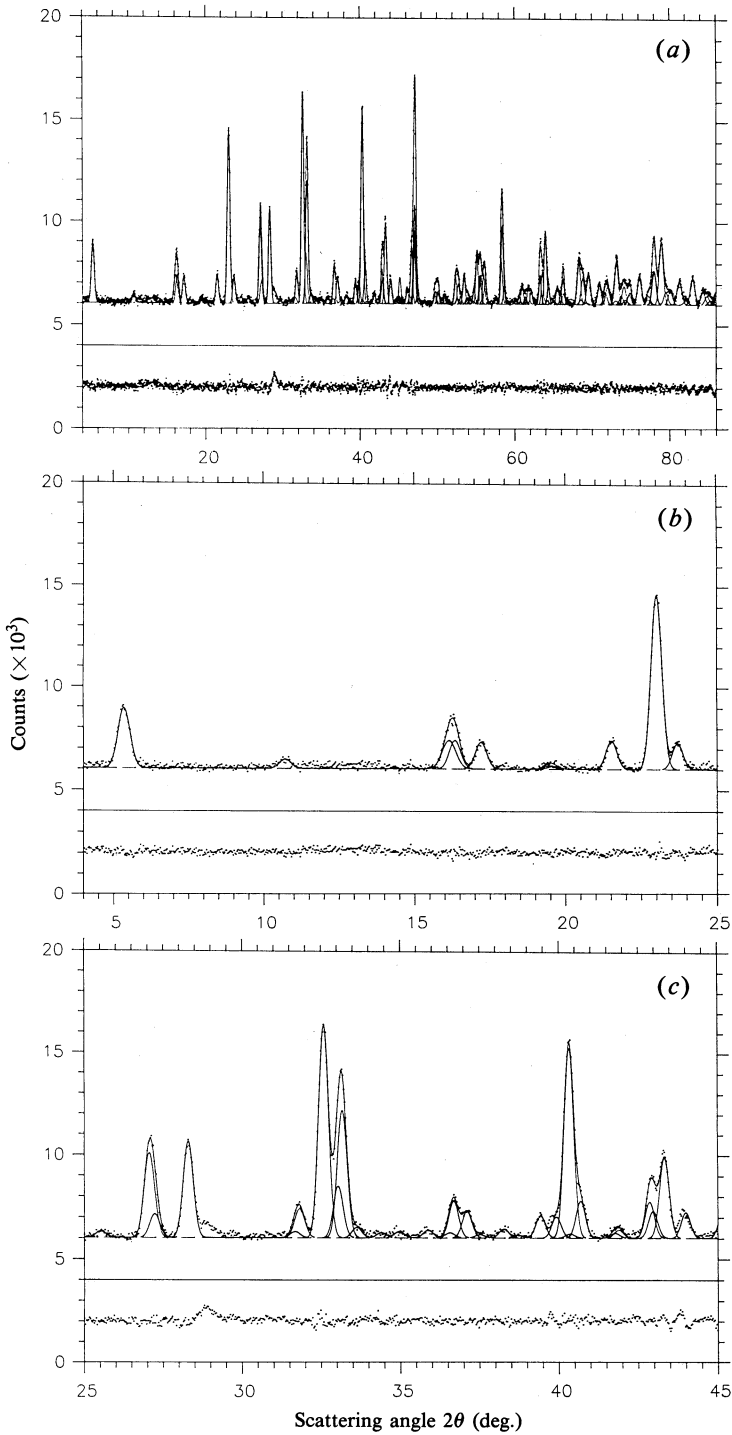


Fig. 9. Neutron diffraction diagrams of the new superconducting compound $\text{YBa}_2\text{Cu}_3\text{O}_{6.9}$ analysed with FULFIT (R profile of 1.2%): (a) shows the full diagram, while (b) and (c) show sections where the individual peaks can be clearly seen.

(d) *Profile Analysis on the New Superconductor $YBa_2Cu_3O_{8-y}$*

The real test of the method comes when unknown materials have to be investigated. In the newly found superconducting compound $YBa_2Cu_3O_{8-y}$, we are confronted with such a problem. Since the first reports of the superconducting properties of this material many diffraction patterns and many studies have been made. Since no single crystals are available the analysis has to be based on powder diffraction data. We have no synchrotron X-ray diffraction diagrams; however, we were able to run three samples from independent sources by neutron diffraction. One is depicted in Fig. 9. As a first step we have performed profile analysis on this diagram and the result is indicated by the solid curves. In the diffraction range accessible we could extract about 200 peaks, many of them well separated and others extracted by profile analysis. They can be used for Fourier calculations and difference Fourier maps in order to find the exact oxygen positions, and finally for least squares refinement in order to determine the occupancy numbers and from that the composition of this nonstoichiometric compound.

Acknowledgments

I am indebted to Dr Parrish, IBM Research Laboratory, San Jose, and his coworkers for the opportunity to work with him and use data from runs on the Stanford Synchrotron facilities. Further, I also thank my colleagues in Bonn and Jülich, Drs Elf, Jansen and Schäfer for the software development on profile analysis. The analysis of the superconductor is a special example of the power of profile fitting. It has been done by E. Jansen. Finally I thank Dr N. Masciocchi and Dr M. Bellotto who I worked with during a stay at the IBM Research Laboratory at San Jose. This work has been funded in part by the German Federal Ministry for Research and Technology (BMFT) under contract 03W11 BON.

References

- Cagliotti, G., Paoletti, A., and Ricci, F. P. (1958). *Nucl. Instrum. Methods* 3, 223–8.
Coppens, P. (1977). *Angew. Chem. Int. Ed. Engl.* 16, 32–40.
Cromer, D. T., and Liberman, D. (1970). *J. Chem. Phys.* 53, 1891–8.
Cromer, D. T., and Liberman, D. (1981). *Acta Cryst. A* 37, 267–8.
Hastings, J. B., Thomlinson, W., and Cox, D. E. (1984). *J. Appl. Cryst.* 17, 85–95.
Huang, T. C., and Parrish, W. (1975). *Appl. Phys. Lett.* 27, 123–4.
Jansen, E., Schaefer, W., and Will, G. (1988). Profile fitting and two-stage method in neutron powder diffraction for structure and texture analysis. *J. Appl. Cryst.* 21 (in press).
Kirfel, A., and Will, G. (1980). *Acta Cryst. B* 36, 512–23.
Ramaseshan, S., and Abrahams, S. C. (1975). 'Anomalous Scattering' (Munksgaard: Copenhagen).
Rietveld, H. M. (1967). *Acta Cryst.* 22, 151–2.
Rietveld, H. M. (1969). *J. Appl. Cryst.* 2, 65–71.
Saiki, A., Ishizawa, N., Mizutani, N., and Kato, M. (1985). *J. Ceram. Soc. Jpn* 93, 649–54.
Savitzky, A., and Golay, M. (1964). *Anal. Chem.* 36, 1627–39.
Steenstrup, S. (1981). *J. Appl. Cryst.* 14, 226–9.
Steinier, J., Termonia, Y., and Deltour, J. (1972). *Anal. Chem.* 44, 1906–9.
Templeton, D. H., Templeton, L. K., Philips, J. C., and Hodgson, K. O. (1980). *Acta Cryst. A* 36, 436–42.
Templeton, L. K., Templeton, D. H., Phizackerley, R. P., and Hodgson, K. O. (1982). *Acta Cryst. A* 38, 74–8.
Will, G. (1979). *J. Appl. Cryst.* 12, 483–5.

- Will, G., Bellotto, M., Parish, W., and Hart, M. (1988). *J. Appl. Cryst.* **21**, (in press).
- Will, G., Jansen, E., and Schaefer, W. (1983*a*). POWLS-80: a program for calculation and refinement of powder diffraction data. Report Juel-1867, KFA Juelich.
- Will, G., and Lauterjung, J. (1987). Proc. US-Japan Seminar on High Pressure Research Applications in Geophysics and Geochemistry (Eds M. H. Manghnani and Y. Syono), pp. 177-86 (Am. Geophys. Union: Washington, DC).
- Will, G., Masciocchi, N., Hart, M., and Parrish, W. (1987*a*). *Acta Cryst. A* **43**, 677-83.
- Will, G., Masciocchi, N., Parrish, W., and Hart, M. (1987*b*). *J. Appl. Cryst.* **20**, 394-401.
- Will, G., Parrish, W., and Huang, T. C. (1983*b*). *J. Appl. Cryst.* **16**, 611-22.
- Young, R. A., and Wiles, D. B. (1982). *J. Appl. Cryst.* **15**, 430-8.

Manuscript received 21 August 1987, accepted 13 January 1988